Neodymium Magnet Rotating Speed-assisted Cu Electroplating In Sulfate Solution Over An Al Alloy Substrate To Enhance Corrosion Resistance, Hardness Characteristics, And Antibacterial Properties

Basori[1*], Ruliyanta[2], Maman Kartaman Ajiriyanto[3], Juan Carlos Sihotang[3], Yusuf Gigih Wicaksono[3], Sigit Dwi Yudanto[4], Evi Ulina Margareta Situmorang[5], Daniel Edbert[6], Cahaya Rosyidan[7], Dwi Nanto[8], and Ferry Budhi Susetyo[9]

[1] *Department of Mechanical Engineering, Universitas Nasional, Jakarta, 12520, Indonesia*
[2] *Department of Electrical Engineering, Universitas Nasional, Jakarta, 12520, Indonesia*
[3] *Research Center for Nuclear Material and Radioactive Waste Technology, National Research and Innovation Agency, Tangerang Selatan, Banten, 15314, Indonesia*
[4] *Research Center for Metallurgy, National Research and Innovation Agency, Tangerang Selatan, Banten, 15314, Indonesia*
[5] *Department of Physiology School of Medicine and Health Sciences, Atma Jaya Catholic University of Indonesia, Jakarta, 14440, Indonesia*
[6] *Department of Microbiology School of Medicine and Health Sciences Atma Jaya Catholic University of Indonesia, Jakarta, 14440, Indonesia*
[7] *Department of Petroleum Engineering, Universitas Trisakti, Jakarta, 11440, Indonesia*
[8] *Department of Physics Education, UIN Syarif Hidayatullah, Jakarta, 15412, Indonesia*
[9] *Department of Mechanical Engineering, Universitas Negeri Jakarta, Jakarta, 13220, Indonesia*
[*] *Corresponding author. E-mail: basori@civitas.unas.ac.id*

Received: Dec. 13, 2025; Accepted: Apr. 29, 2026

Copper (Cu) coatings enhance the corrosion resistance, hardness, and antibacterial properties of aluminum (Al). To further optimize these traits, this study electroplated Cu onto an Al alloy under a rotating neodymium magnet at various speeds. The resulting pure, face-centered cubic (FCC) Cu films were comprehensively characterized. Results indicated that increasing the magnetic rotation speed decreased the deposition rate, current efficiency, and crystallite size, while simultaneously increasing the film's hardness, grain size, and corrosion potential. Ultimately, a magnetic rotation of 250 rpm proved optimal, producing a compact Cu film with maximum hardness, corrosion resistance, and bacterial inhibition.

Keywords: surface morphology, crystallographic orientation, sodium chloride, Vickers, gram-positive bacteria

http://dx.doi.org/10.6180/jase.202610_33.018

1. Introduction

Aluminum (Al) alloy is widely used in hospital equipment due to the favorable mechanical properties and ease of forming by the machining process [1, 2]. However, various Al materials can act as vectors for bacteria transmission, as pathogens spread through frequently touched hospital equipment, including push plates, door knobs, tray tables, railings, and tap handles [3]. This condition can be prevented by coating Al using a material with antimicrobial property such as copper (Cu).

Compared to Cu, Al does not possess an intrinsic antibacterial activity [4] but plays an indirect role in influencing the physicochemical properties of composite materials. Al can modify surface charge, enhance material stability, and alter ion release kinetics, thereby modulating the bioavailability and antibacterial efficacy of Cu. A previous study by Hutasoit et al. stated that Al coated with Cu would result in Cu ions being released more than stainless steel (SS) coated using Cu, due to Cu-Al having a negative galvanic potential [5]. This reaction occurs because bacterial activity is influenced by Cu released to the environment.

Among various methods available for coating Al with Cu, electroplating is one of the most widely used due to low cost and ease of controlling the parameters [6]. Major parameters during electroplating include current, electrolyte temperature, and magnetic field influence [7–9]. Generally, these parameters control the arrangement of ion movement to the cathode, which determines the resulting morphology and crystallographic orientation of the deposited coating [10].

During Cu electroplating on Al under the influence of a magnetic field, Cu ions in the solution are affected by multiple forces such as diffusion, convection, Lorentz, and magnetic gradient force. These forces have a significant impact on mass transfer and grain nucleation rate [11]. Specifically, decreasing the rotation of the magnet with a south pole near the cathode will reduce the deposition rate and current efficiency due to multiple forces [12]. Deposition rate and current efficiency strongly depend on the movement of Cu ions to the cathode and hydrogen production, respectively [13–15].

The rate of Cu ion transport to cathode plays a significant role in determining surface morphology, grain size, and crystallographic orientation [7, 12, 16]. A dense surface morphology can improve the barrier effect and enable the protection of the substrate against corrosion attack, thereby increasing corrosion resistance [17]. In addition to morphology, crystallographic orientation, particularly crystallite size, also affects the mechanical properties and bacterial activity, which influence hardness and area of inhibition. This is because the lowest crystallite size will produce the highest hardness and the highest inhibition area [18, 19]. Moreover, higher hardness corresponds to the elevated dislocation density, which increases Cu ion diffusion and microbial killing efficiency [5].

Despite the established relationships, there is still a limited report on the influence of the rotating magnetic field during Cu electroplating [12, 20–22], as several studies have mainly focused on the unrotated magnetic field [7, 9, 23, 24]. According to a previous study, different spinning rates (0,50 , and 100 rpm) cause variations in corrosion resistance, hardness characteristics, and antibacterial properties [12]. Higher rotation of the south-pole magnet near the cathode has also been reported to enhance antibacterial activity and corrosion resistance.

Based on the description above, this study aims to investigate Cu electroplating on Al alloy under rotating neodymium magnet conditions (south-pole magnet near the cathode) at various speeds. The main objective is to understand the influence of spinning speed exceeding 100 rpm on deposition rate, current efficiency, surface morphology, elements, and crystallographic orientation. The physical properties are correlated to electrochemical behavior, bacterial activity, and average hardness. The selected spinning speed of 150, 200, and 250 rpm are adopted based on a previous study using multiples of 50 rpm [12].

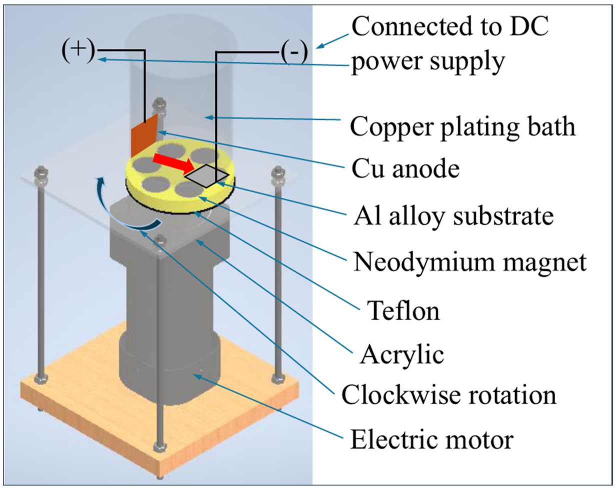

Fig. 1. Rotating magnetic influence apparatus [12].

2. Materials and methods

2.1. Material and Sample Synthesis

Al alloy ($20 \times 20 \times 2$ mm) was used as substrate, Cu as anode ($50 \times 50 \times 2$ mm), and the electroplating bath ($0.5 MCuSO_4 + 20 mlH_2SO_4$) was prepared following the procedures reported in a previous study [12]. Electroplating was performed using a Power Supply (MDB PS-305DM) at 120 mA for one hour. During electroplating, a spinning neodymium magnet was used to influence the movement of Cu ions. Subsequently, three pieces of neodymium magnet were stacked, embedded, and arranged on the upper side of the Teflon (South pole near the plating bath) as shown in Fig. 1 [12]. Electroplating conditions were varied, including the speed of the spinning magnet, 150, 200, and 250 rpm for Cu-150, Cu-200, and Cu-250, respectively. Before and after electroplating, the sample was weighed to measure the deposition rate and current efficiency [12].

2.2. Characterizations

The surface morphology and elements were investigated using a scanning electron microscope equipped with energy dispersive spectroscopy (SEM-EDS), JEOL (JSM-6510 LA). Moreover, crystallographic orientation was measured using X-ray diffraction (XRD), Panalytical. The measured XRD data were refined with the GSAS software [25]. The average crystallite size was calculated using the Debye-Scherrer formula, as presented in Equation 1 [26].

$$D = k\lambda/\beta \cdot \cos\theta \quad (1)$$

where, D is the average crystal size (nm), k is the shape constant (k = 0.9), λ is the X-ray radiation wavelength (Cu$k\alpha$ = 0.15406 nm), β is the full width at half maximum (FWHM) value (°), and θ is the crystal plane's peak position (°).

The electrochemical study was conducted using a Potentiostat (Ossila) in 60 ml of 0.9% NaCl at room temperature. A 1 cm^2 Cu layer was exposed in a chloride solution as the working electrode, Pt as the counter electrode, and Ag/AgCl as the reference electrode. Before potentiodynamic polarization (PP) measurement using 5mV/s (between -1.0 and 0.5 V), an open circuit potential (OCP) was applied for 1500 seconds. Moreover, the PP data were extrapolated using the Tafel method, and the corrosion rate was calculated using a method similar to that used in the previous study [9].

The hardness was measured with microhardness (LECO-LM 800 A) using 100 g for 15 seconds of dwell time. A total of four repeatable hardness measurements were conducted at room temperature, and bacteria activity was tested using Staphylococcus aureus ATCC 25923 (gram-positive bacteria). The test was incubated at 35 ± 2°C for 24 hours, followed by measuring the kill and inhibition areas using Image-J software.

3. Results and discussions

3.1. Deposition Rate and Current Efficiency

Fig. 2 shows the variation in deposition rate and current efficiency during Cu electroplating induced by a spinning magnet. By increasing the spinning speed, the leading deposition rate and current efficiency decreased. Based on observation, a lower deposition rate indicates that poor ions are placed over the cathode [9, 13], while a decrease in current efficiency suggests an increase in discharge of H^+ions over the cathode [14]. The deposition rate and current efficiency vary from 39.62 to 37.95μm/h and 99.81 to 95.59%, respectively.

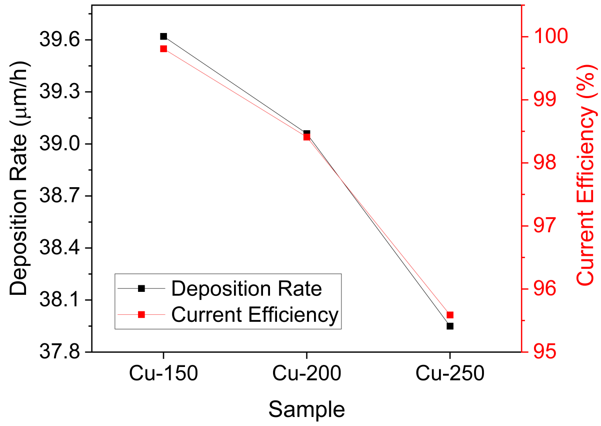

Fig. 2. Deposition rate and current efficiency during electroplating were induced by various spin rates of a neodymium magnet.

Generally, the magnetic field inducing the electrochemical process can affect a larger amount of hydrogen produced [27, 28]. Enhancing the magnetic field intensity can also decrease the deposition rate and current efficiency due to more hydrogen being produced over the cathode [9]. According to Fig. 2, both deposition rate and current efficiency decreased with increasing speed of magnetic rotation. This is due to high production of hydrogen during electroplating, thereby hydrogen bubbles disrupt the movement of Cu ions. A previous study by Guo et al. stated that the rise in magnetic rotation caused a significant increase in hydrogen production [15]. Moreover, hydrogen could also influence the kinetic layer growth by acting as an obstacle to Cu ion movement [29].

3.2. SEM-EDS

SEM of various samples presented in Fig. 3 shows a non-uniform surface morphology structure [30]. This indicates that increasing magnet spinning did not make the surface morphology uniform. However, dense surface morphology was observed in Cu-250, which was influenced by the highest spinning speed during electroplating. EDS was also conducted, as shown in Fig. 3, where Cu element was identified in various samples, and other impurities were not presented. However, some previous studies reported the presence of carbon (C), oxygen (O), or sulfur (S) elements [31, 32]. Although other impurities were not found, Cu was identified as an element on the sample surface, indicating successful plating onto the Al alloy surface.

According to the SEM image, grain distribution using Image-J followed by Origin software was conducted, with results shown in Fig. 3. Based on observation, increasing spinning speed caused a shift to wider grain sizes. A sig-

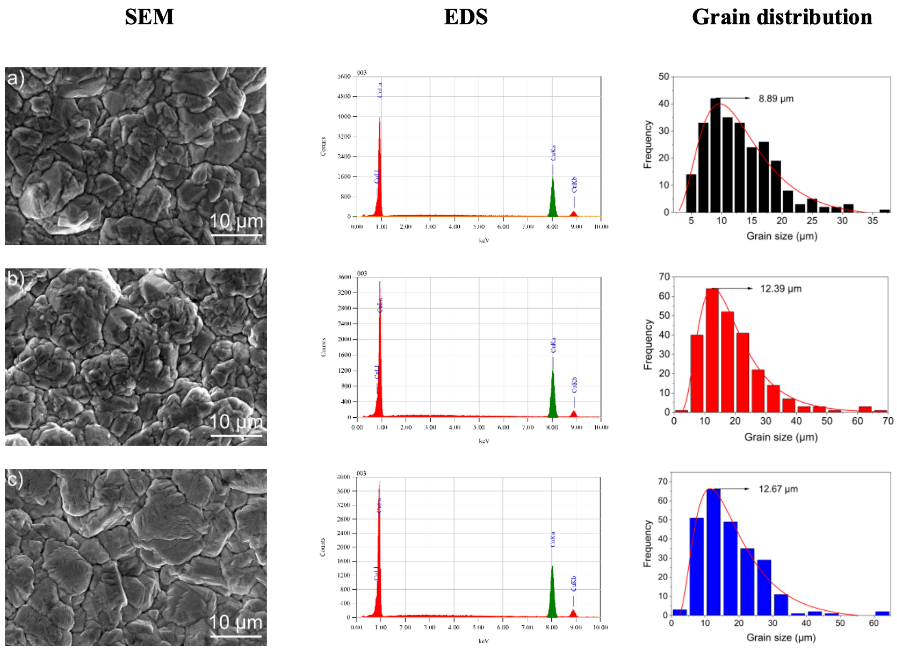

Fig. 3. SEM-EDS and Grain distribution of electroplated samples (a) Cu-150, (b) Cu-200, and (c) Cu-250.

nificant increase occurred when the rotating speed rose from 150 to 200 rpm, with grain size from 8.89 to 12.39μm. Increasing the rotating speed to 250 rpm caused a change of approximately 0.28μm. The formation of larger grain sizes was found to be influenced by nucleation rate, as a lower rate led to broader grain size [7, 16]. Moreover, a decrease in grain size could raise many grain boundaries, acting as a barrier to dislocation motion [33].

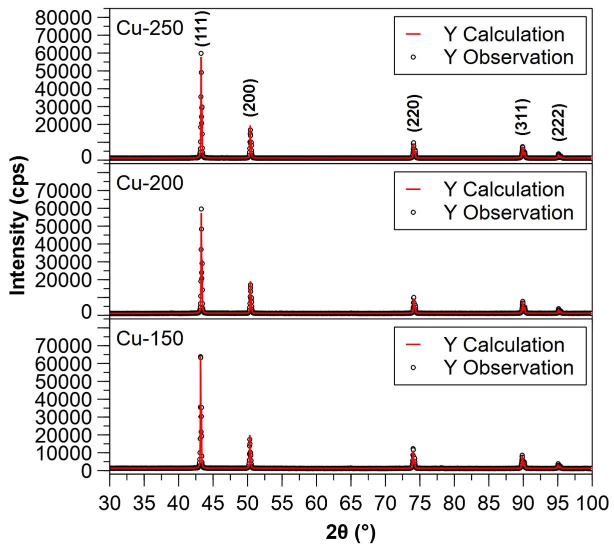

Fig. 4. Diffraction pattern of Cu electroplating induced by a spinning magnet with various rotation rates.

3.3. X-ray Diffraction

Fig. 4 shows the calculated diffraction patterns of electroplated Cu samples with varying magnetic rotation, which are fitted with the observed results. The FCC Cu phase, corresponding with ICDD PDF-5 number #004-0836, was found by X-ray reflections on crystal planes (111), (200), (220), (311), and (222). This phase has peaks that are comparable to the values reported by Phul et al. [34]. Qualitatively, the speed of magnetic rotation did not affect the formation of other phases. Based on the lattice constant -a value of 0.3615 nm for the cubic Cu phase, Rietveld method calculations showed that the three samples had no lattice distortion.

In line with the analysis, enhancing the rotation speed caused the average crystallite size to be refined from 93 to 87 nm. These results are consistent with a previous study, where increasing the magnetic spinning speed leads to a reduced crystallite size [12]. Moreover, the crystallographic data of Cu samples electroplated with variations in magnetic rotation are shown in Table 1.

3.4. Electrochemical behavior

Electrochemical behavior was tested in a 0.9 % NaCl solution at room temperature. Specifically, NaCl was selected because eccrine sweat and saline-infused solutions contained 0.9 % NaCl [20]. In the medical equipment, exposure to these two materials can cause corrosion. Prior to PP, the OCP was monitored for 1500 seconds. Based on

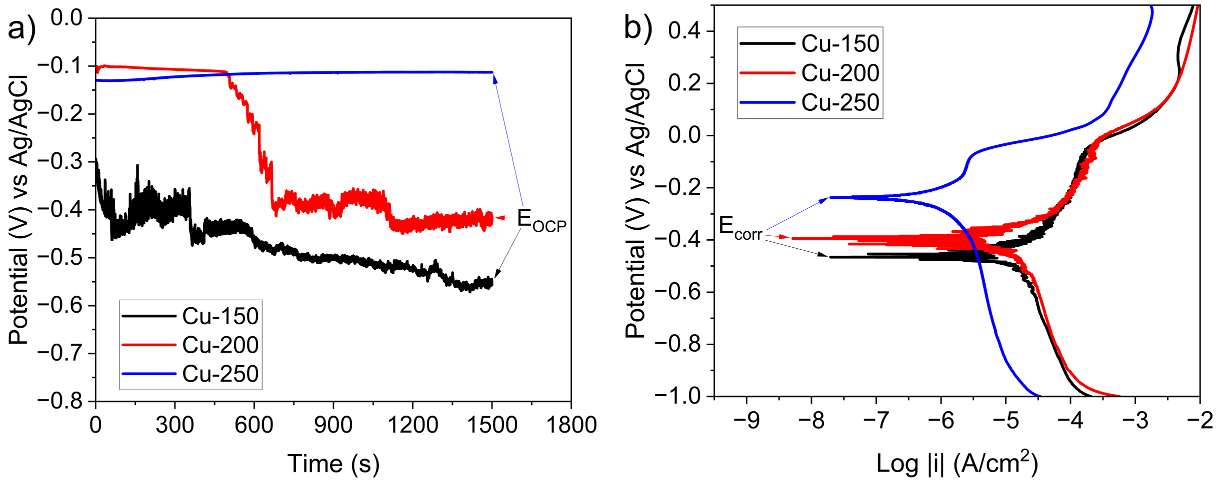

Fig. 5. Electrochemical behavior of electroplated samples (a) OCP and (b) PP.

Table 1. Diffraction refinement results of **Cu** electroplating induced by a spinning magnet with various rotation rates

Source	Cu-150	Cu-200	Cu-250
Crystallography	Name: Cu System crystal: cubic Space group: fm-3m (225)		
Lattice constant -a (nm)	0.3615	0.3615	0.3615
FWHM (111) (°)	0.072	0.077	0.075
FWHM (200) (°)	0.087	0.090	0.091
FWHM (220) (°)	0.124	0.128	0.136
FWHM (311) (°)	0.159	0.161	0.174
Average crystallite size (nm)	93	89	87

observation, Al substrate tends to shift both the E_{OCP} and corrosion potential of Cu films towards more negative values. Sadawy et al. reported a corrosion potential of Cu in 3.5 NaCl is -0.240 (V) vs Ag/AgCl [35], while Samura et al. conducted an electrochemical study of Cu in 0.9 % NaCl and found that E_{OCP} at 1200 seconds measurement -0.014(V) vs Ag/AgCl, and corrosion potential was -0.241 (V) vs Ag/AgCl [36]. When compared with previous reports, this study has a more negative E_{OCP} and corrosion potential.

As presented in Fig. 5 (a), the OCP measurement showed that Cu -150 and Cu -200 samples shifted toward more negative values until 1500 seconds, while Cu − 250 showed a movement to more positive values by increasing time consumption. Moreover, Cu-150 samples produced a more negative E_{OCP} tendency than other samples at the end of the measurement. A more positive value of the E_{OCP} indicates a higher driving force for reduction, suggesting a significant increase in line with the rising magnetic spinning rate [37]. The complete E_{OCP} values are summarized in Table 2.

The trend of OCP curve shows surface film behavior. A shift toward more positive value indicates the formation of an oxide film on the surface, while a negative value suggests dissolution of the oxide film and the formation of CuCl film [38, 39]. This suggests that Cu 250 sample

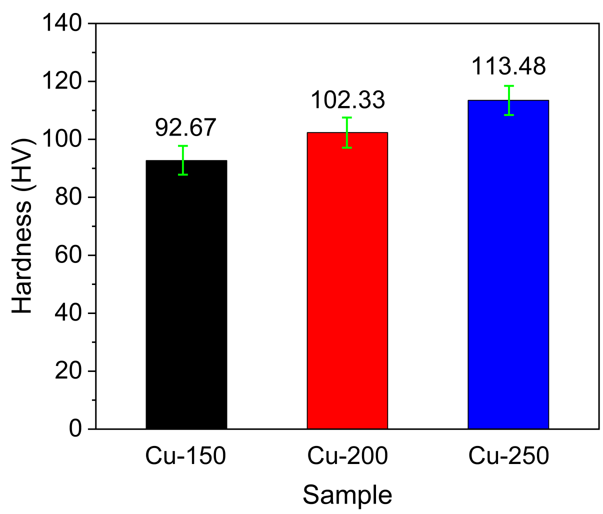

Fig. 6. Average microhardness of various Cu films.

has a continuous form of Cu oxide until 1500 seconds of measurement. In comparison, Cu -150 and Cu -200 samples show the occurrence of dissolution of the Cu oxide in the 0.9%NaCl solution.

Fig. 5 (b) shows PP measurement in the 0.9%NaCl solution. In this study, the Tafel extrapolation method was used to determine corrosion potential (E_{corr}) and corrosion current (i_{corr}), with results shown in Table 2. Corrosion rate was calculated using a method similar to the strategy used in a previous study [12].

As shown in Table 2, more rotation of the magnetic field was observed to cause a reduction in corrosion rate. This behavior is associated with the quality and characteristics of the deposited Cu film. According to Kim et al., OCP is an indicator of corrosion potential that can identify corrosion behavior [39]. When compared with the OCP results, the Cu-250 sample showed a continuous shift toward a more positive direction, indicating oxide formation. This oxide layer acts as a protective barrier against aggressive species such as Cl. In addition to oxide formation, the Cu-250 sample also has a dense morphology that can improve the barrier effect and enable the protection of the substrate against corrosion attack [17]. The combined influence of a stable oxide layer and compact morphology results in superior corrosion resistance for the Cu-250 coating. Furthermore, Cu-250 film has a corrosion current of 0.443 $\mu A/cm^2$ in 0.9%NaCl, which is lower than Cu1.95$\mu A/cm^2$ [38].

3.5. Microhardness

The Vickers microhardness test was used to determine the hardness of the samples, with four repeated measurements conducted on top of the Cu layer. The average hardness values presented in Fig. 6 ranged from 92.67 to 113.48 HV. A previous study conducted by Ibrahim and Bakdash found Cu film hardness between 96-97 HV when electroplated Cu at various temperatures ($20 - 40°C$) [40]. Moreover, at static conditions, presenting a magnetic field promotes an increase in the hardness [41].

As shown in Fig. 6, increasing the magnetic rotation speed further improves the hardness of the Cu layer due to changes in crystallite size. According to Wagih and Shaat, crystallite size is the main factor influencing the mechanical properties, including the hardness of the material [42]. This is because the lowest crystallite size will produce the highest hardness [18]. Compared to the XRD refinement, increasing the spinning rate leads to a reduction in crystallite size, which contributes to the observed improvement in hardness.

3.6. Antibacterial Test

Fig. 7 (a) shows the kill and inhibition areas of various samples subjected to Staphylococcus aureus ATCC 25923 bacteria. The area of inhibition is shown between the red and blue lines in Fig. 7 (b), while the kill area is inside the red line. The higher areas are presented in the Cu-250 sample, while the lowest is observed in Cu-200. In comparison, the difference observed between 150 and 200 rpm samples suggests that lower spinning rates have only a limited effect on antibacterial performance, which can be attributed to similarities in the resulting surface morphology [43]. Attributed to the release of Cu ions to the environment, more ions released could more effectively inhibit bacterial growth [32]. As shown in Fig. 3, the Cu-250 has a denser surface morphology than the other sample.

Several studies have found that antibacterial efficiency is influenced by coating hardness [44–46]. Hutasoit et al. have found that higher hardness corresponded to a greater dislocation density, causing an increase in Cu ion diffusion and microbial killing efficiency [5]. According to Figure 6, higher hardness was observed in Cu-250 sample, which enhanced the kill and inhibition areas. Cu-250 also has the lowest crystallite size, which produces the highest inhibition area [19]. Syamsuir et al. also found that a smaller crystallite size of the Cu film would lead to a larger area of inhibition [20]. This behavior is due to the lowest crystallite size, causing a larger surface area [47], with high release of Cu ions and a greater inhibition area.

4. Conclusions

In conclusion, this study successfully synthesizes Cu electroplating under various spinning rates of magnetic influence. The results show that the magnetic spinning rates influence deposition rate, current efficiency, surface morphology, grain size, crystallite size, corrosion resistance, hardness, and area of inhibition. An increase in magnetic rotating rate lead to poor placement of Cu ions on the cathode and high discharge of H^+ions, thereby reducing the deposition rate and current efficiency. In comparison, a decrease in deposition rate leads to low nucleation rate, causing an increase in grain size and denser surface morphology, which contributes to a higher corrosion resistance of Cu film. Moreover, a rise in magnetic spinning rate promotes a decrease in crystallite size, which increase the hardness of Cu films. Higher hardness, associated with increased dislocation density and enhanced Cu ion diffusion, leads to improved microbial killing efficiency and a larger inhibition area. Moreover, future studies are recommended to optimize Cu electroplating induced by speed rotation exceeding 250 rpm , with varying neodymium magnets of

Table 2. Electrochemical behavior result

Samples	E_{corr} (V) vs Ag/AgCl	i_{corr} ($\mu A/cm^2$)	Corrosion rate (mm/y)	E_{ocp} (V) vs Ag/AgCl
Cu-150	-0.462	4.857	5.63×10^{-2}	-0.556
Cu-200	-0.397	3.814	4.42×10^{-2}	-0.421
Cu-250	-0.237	0.443	5.14×10^{-3}	-0.113

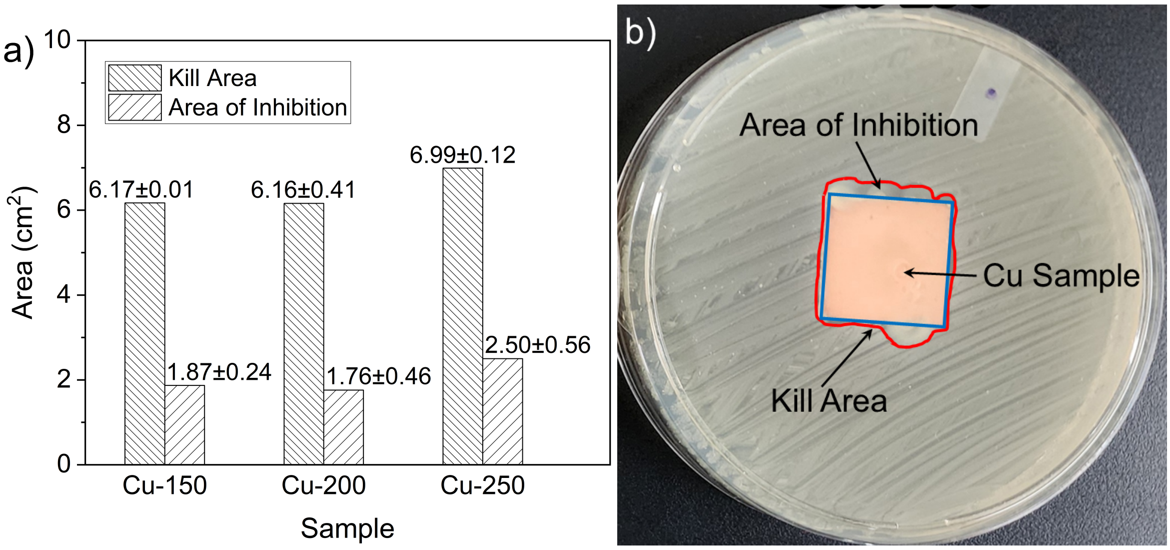

Fig. 7. Antibacterial test result of electroplated samples (a) Kill area and area of inhibition, and (b) Cu-250 sample kill area and area of inhibition visualization.

more than three pieces.

Acknowledgements

This project receives financial support from the Ministry of Higher Education, Science and Technology, Republic of Indonesia, under contract numbers 124/C3/DT.05.00/PM/2025 and 0995/LL3/AL.04/2025, 101/LPPM-UNAS/VI/2025.

References

[1] D. Y. Pimenov, M. Kiran, N. Khanna, G. Pintaude, M. C. Vasco, L. R. R. da Silva, and K. Giasin, (2023) *"Review of improvement of machinability and surface integrity in machining on aluminum alloys"* **The International Journal of Advanced Manufacturing Technology** ***129***: 4743–4779. DOI: 10.1007/s00170-023-12630-4.

[2] C.-R. Song, B.-X. Dong, S.-Y. Zhang, H.-Y. Yang, L. Liu, J. Kang, J. Meng, C.-J. Luo, C.-G. Wang, K. Cao, J. Qiao, S.-L. Shu, M. Zhu, F. Qiu, and Q.-C. Jiang, (2024) *"Recent progress of Al–Mg alloys: Forming and preparation process, microstructure manipulation and application"* **Journal of Materials Research and Technology** ***31***: 3255–3286. DOI: 10.1016/j.jmrt.2024.07.051.

[3] A. Augustin, P. Huilgol, K. R. Udupa, and U. Bhat K, (2016) *"Effect of current density during electrodeposition on microstructure and hardness of textured Cu coating in the application of antimicrobial Al touch surface"* **Journal of the Mechanical Behavior of Biomedical Materials** ***63***: 352–360. DOI: 10.1016/j.jmbbm.2016.07.013.

[4] J. H. Reed, A. E. Gonsalves, J. K. Román, J. Oh, H. Cha, C. E. Dana, M. Toc, S. Hong, J. B. Hoffman, J. E. Andrade, K. D. Jo, M. Alleyne, N. Miljkovic, and D. M. Cropek, (2019) *"Ultrascalable Multifunctional Nanoengineered Copper and Aluminum for Antiadhesion and Bactericidal Applications"* **ACS Applied Bio Materials** ***2***: 2726–2737. DOI: 10.1021/acsabm.8b00765.

[5] N. Hutasoit, S. H. Topa, M. A. Javed, R. A. Rahman Rashid, E. Palombo, and S. Palanisamy, (2021) *"Antibacterial Efficacy of Cold-Sprayed Copper Coatings against Gram-Positive Staphylococcus aureus and Gram-Negative Escherichia coli"* **Materials** ***14***: 6744. DOI: 10.3390/ma14226744.

[6] A. Lelevic and F. C. Walsh, (2019) *"Electrodeposition of Ni P alloy coatings: A review"* **Surface and Coatings Technology** ***369***: 198–220. DOI: 10.1016/j.surfcoat.2019.03.055.

[7] H. A. Murdoch, D. Yin, E. Hernández-Rivera, and A. K. Giri, (2018) *"Effect of applied magnetic field on microstructure of electrodeposited copper"* **Electrochemistry Communications *97***: 11–15. DOI: 10.1016/j.elecom.2018.09.013.

[8] X. Fu, C. Zhan, R. Zhang, B. Wang, H. Sun, and J. Sun, (2022) *"Effect of temperature on mechanism and kinetics of electrochemical nucleation of copper in ChCl-based deep eutectic solvents"* **Journal of Solid State Electrochemistry *26***: 2713–2722. DOI: 10.1007/s10008-022-05282-z.

[9] B. Soegijono, F. B. Susetyo, Yusmaniar, and M. C. Fajrah, (2020) *"Electrodeposition of Paramagnetic Copper Film under Magnetic Field on Paramagnetic Aluminum Alloy Substrates"* **e-Journal of Surface Science and Nanotechnology *18***: 281–288. DOI: 10.1380/ejssnt.2020.281.

[10] Y. Mo, C. Shen, and D. Zhu, (2022) *"Study of Copper Electrodeposition at a Very Low Temperature near the Freezing Point of Electrolyte"* **Micromachines *13***: 2225. DOI: 10.3390/mi13122225.

[11] Q. Long, Y. Zhong, and J. Wu, (2020) *"Research Progress of Magnetic Field Techniques for Electrodeposition of Coating"* **International Journal of Electrochemical Science *15***: 8026–8040. DOI: 10.20964/2020.08.40.

[12] B. Basori, Ruliyanta, M. K. Ajiriyanto, R. Kriswarini, H. Hardiyanti, C. Rosyidan, S. D. Yudanto, E. U. M. Situmorang, D. Edbert, D. Nanto, and F. B. Susetyo, (2025) *"Rotating speed and magnetic pole dependency assisted on copper deposition onto aluminum alloy substrate for bacterial eradication application"* **Communications in Science and Technology *10***: 17–28. DOI: 10.21924/cst.10.1.2025.1547.

[13] B.-N. Park, Y.-S. Sohn, and S.-Y. Choi, (2008) *"Effects of a magnetic field on the copper metallization using the electroplating process"* **Microelectronic Engineering *85***: 308–314. DOI: 10.1016/j.mee.2007.06.018.

[14] M. F. Alebrahim, I. Khattab, and A. O. Sharif, (2015) *"Electrodeposition of copper from a copper sulfate solution using a packed-bed continuous-recirculation flow reactor at high applied electric current"* **Egyptian Journal of Petroleum *24***: 325–331. DOI: 10.1016/j.ejpe.2015.07.009.

[15] H. Guo, H.-J. Kim, and S.-Y. Kim, (2022) *"Research on Hydrogen Production by Water Electrolysis Using a Rotating Magnetic Field"* **Energies *16***: 86. DOI: 10.3390/en16010086.

[16] G. Yamaguchi and H. Mimura, (2020) *"Effect of Electrodeposition Conditions on Surface Roughness of Copper Electroformed Replicas"* **International Journal of Electrical Machining *25***: 33. DOI: 10.2526/ijem.25.33.

[17] F. da Silva, N. Cinca, S. Dosta, I. Cano, J. Guilemany, C. Caires, A. Lima, C. Silva, S. Oliveira, A. Caires, and A. Benedetti, (2019) *"Corrosion resistance and antibacterial properties of copper coating deposited by cold gas spray"* **Surface and Coatings Technology *361***: 292–301. DOI: 10.1016/j.surfcoat.2019.01.029.

[18] S. Aghamiri, N. Oono, S. Ukai, R. Kasada, H. Noto, Y. Hishinuma, and T. Muroga, (2018) *"Microstructure and mechanical properties of mechanically alloyed ODS copper alloy for fusion material application"* **Nuclear Materials and Energy *15***: 17–22. DOI: 10.1016/j.nme.2018.05.019.

[19] A. Azam, A. S. Ahmed, M. Oves, M. Khan, and A. Memic, (2012) *"Size-dependent antimicrobial properties of CuO nanoparticles against Gram-positive and -negative bacterial strains"* **International Journal of Nanomedicine *7***: 3527–3535. DOI: 10.2147/ijn.s29020.

[20] S. Syamsuir, F. B. Susetyo, B. Soegijono, S. D. Yudanto, B. Basori, M. K. Ajiriyanto, D. Edbert, E. U. M. Situmorang, D. Nanto, and C. Rosyidan, (2023) *"Rotating-Magnetic-Field-Assisted Electrodeposition of Copper for Ambulance Medical Equipment"* **Automotive Experiences *6***: 290–302. DOI: 10.31603/ae.9067.

[21] I. Mogi, R. Morimoto, R. Aogaki, and K. Takahashi, (2019) *"Surface Chirality in Rotational Magnetoelectrodeposition of Copper Films"* **Magnetochemistry *5***: 53. DOI: 10.3390/magnetochemistry5030053.

[22] I. Mogi, R. Morimoto, R. Aogaki, and K. Watanabe, (2013) *"Surface chirality induced by rotational electrodeposition in magnetic fields"* **Scientific Reports *3***: 2574. DOI: 10.1038/srep02574.

[23] Y. Liu, B. Zheng, T. Zhang, Y. Chen, J. Liu, Z. Wang, and X. Gong, (2022) *"Magnetic field intensified electrodeposition of low-concentration copper ions in aqueous solution"* **Electrochimica Acta *432***: 141201. DOI: 10.1016/j.electacta.2022.141201.

[24] D. in, H. A. Murdoch, B. Chad Hornbuckle, E. Hernández-Rivera, and M. K. Dunstan, (2019) *"Investigation of anomalous copper hydride phase during magnetic field-assisted electrodeposition of copper"* **Electrochemistry Communications *98***: 96–100. DOI: 10.1016/j.elecom.2018.11.018.

[25] B. H. Toby and R. B. Von Dreele, (2013) *"<i>GSAS-II</i>: the genesis of a modern open-source all purpose crystallography software package"* **Journal of Applied Crystallography *46***: 544–549. DOI: 10.1107/s0021889813003531.

[26] R. SEAKR, (2017) *"Microstructure and crystallographic characteristics of nanocrystalline copper prepared from acetate solutions by electrodeposition technique"* **Transactions of Nonferrous Metals Society of China *27***: 1423–1430. DOI: 10.1016/s1003-6326(17)60164-x.

[27] M. Zielinski, (2016) *"Positive and Negative Aspects of Electrode Reactions of Hydrogen Evolution and the Influence of a Constant Magnetic Field"* **Journal of Advanced Chemical Engineering *4***: 1000106. DOI: 10.4172/2090-4568.1000106.

[28] Y.-J. Chen, Y.-H. Li, and C.-Y. Chen, (2022) *"Studying the Effect of Electrode Material and Magnetic Field on Hydrogen Production Efficiency"* **Magnetochemistry *8***: 53. DOI: 10.3390/magnetochemistry8050053.

[29] V. Grozovski, S. Vesztergom, G. G. Láng, and P. Broekmann, (2017) *"Electrochemical Hydrogen Evolution: H⁺or H₂O Reduction? A Rotating Disk Electrode Study"* **Journal of The Electrochemical Society *164***: E3171–E3178. DOI: 10.1149/2.0191711jes.

[30] H. Matsushima, A. Bund, W. Plieth, S. Kikuchi, and Y. Fukunaka, (2007) *"Copper electrodeposition in a magnetic field"* **Electrochimica Acta *53***: 161–166. DOI: 10.1016/j.electacta.2007.01.043.

[31] I. Mladenović, J. Lamovec, D. Vasiljević Radović, V. Radojević, and N. D. Nikolić, (2022) *"Influence of intensity of ultrasound on morphology and hardness of copper coatings obtained by electrodeposition"* **Journal of Electrochemical Science and Engineering *12***: 603–615. DOI: 10.5599/jese.1290.

[32] M. Xia, L. Lai, M. Fu, Y. Wu, S. Chen, and G. Liu, (2025) *"Electrodeposition of antibacterial, anti-corrosion copper nanopillars arrays with heat conductive properties for marine environments"* **Journal of Materials Science & Technology *232***: 89–102. DOI: 10.1016/j.jmst.2024.12.087.

[33] C. Wu, X. Ren, L. Xie, W. Wu, Z. Liu, W. Zhai, and J. Wang, (2025) *"Grain refining in copper foil induced by ultrasonic field during the electrodeposition process"* **Ultrasonics Sonochemistry *121***: 107526. DOI: 10.1016/j.ultsonch.2025.107526.

[34] R. Phul, C. Kaur, U. Farooq, and T. Ahmad, (2018) *"Ascorbic acid assisted synthesis, characterization and catalytic application of copper nanoparticles"* **Material Science & Engineering International Journal 2**: 90–94. DOI: 10.15406/mseij.2018.02.00040.

[35] M. Sadawy, S. M. Fayed, M. Tayea, and I. El-Batanony, (2024) *"Microstructure, corrosion and electrochemical properties of Cu/SiC composites in 3.5 wt% NaCl solution"* **Metals and Materials International *30***(3): 568–584. DOI: 10.1007/s12540-023-01521-8.

[36] L. Samura, M. Maulani, C. Rosyidan, K. F. Hartono, S. Prakoso, E. U. M. Situmorang, D. Edbert, B. Soegijono, M. Y. Hasbi, and F. B. Susetyo, (2024) *"Effect of Zinc Addition in Copper to Structure, Hardness, Corrosion, and Antibacterial Activity"* **Journal of Applied Engineering and Technological Science *6***: 465–479. DOI: 10.37385/jaets.v6i1.6098.

[37] C. P. daRosa, E. Iglesia, and R. Maboudian, (2009) *"Copper deposition onto silicon by galvanic displacement: Effect of Cu complex formation in NH4F solutions"* **Electrochimica Acta *54***: 3270–3277. DOI: 10.1016/j.electacta.2008.12.037.

[38] Ž. Z. Tasić, M. B. P. Mihajlović, M. B. Radovanović, and M. M. Antonijević, (2018) *"Electrochemical investigations of copper corrosion inhibition by azithromycin in 0.9% NaCl"* **Journal of Molecular Liquids *265***: 687–692. DOI: 10.1016/j.molliq.2018.03.116.

[39] G.-Y. Kim, J. Jang, J.-H. Woo, S. Yoon, and J.-S. Kim, (2023) *"Electrochemical and surface investigations of copper corrosion in dilute oxychloride solution"* **Nuclear Engineering and Technology *55***(8): 2742–2746. DOI: 10.1016/j.net.2023.05.021.

[40] M. Ibrahim and R. Bakdash, (2015) *"New non-cyanide acidic copper electroplating bath based on glutamate complexing agent"* **Surface and Coatings Technology *282***: 139–148. DOI: 10.1016/j.surfcoat.2015.10.024.

[41] A. Fattahi and M. Bahrololoom, (2015) *"Investigating the effect of magnetic field on pulse electrodeposition of magnetic and non-magnetic nanostructured metals"* **Surface and Coatings Technology *261***: 426–435. DOI: 10.1016/j.surfcoat.2014.10.013.

[42] A. Wagih and M. Shaat, (2019) *"The dependence of accumulative roll bonded copper mechanical properties on grain sub-division, stacking faults, and lattice strains"* **Materials Science and Engineering: A *756***: 190–197. DOI: 10.1016/j.msea.2019.04.061.

[43] J. Fabian, G. Morton, S. Sharma, B. Duffy, and S. Warren, (2025) *"Effect of electrodeposition time on physical characteristics and antibacterial activity of copper-incorporated TiO ₂ nanotubes"* **RSC Advances** ***15***: 142–156. DOI: 10.1039/d4ra05266h.

[44] V. Champagne, K. Sundberg, and D. Helfritch, (2019) *"Kinetically Deposited Copper Antimicrobial Surfaces"* **Coatings** ***9***: 257. DOI: 10.3390/coatings9040257.

[45] V. K. Champagne and D. J. Helfritch, (2013) *"A demonstration of the antimicrobial effectiveness of various copper surfaces"* **Journal of Biological Engineering** ***7***: 8. DOI: 10.1186/1754-1611-7-8.

[46] K. Sundberg, Y. Wang, B. Mishra, A. Carl, R. Grimm, A. Te, L. Lozeau, B. Sousa, R. Sisson, and D. Cote, (2019) *"The Effect of Corrosion on Conventional and Nanomaterial Copper Cold Spray Surfaces for Antimicrobial Applications"* **Biomedical Journal of Scientific & Technical Research** **22**: 16753–16763. DOI: 10.26717/bjstr.2019.22.003768.

[47] G. Kasi, N. Stalin, P. Rachtanapun, K. Jantanasakulwong, J. N. Halder, S. Phongthai, P. Worajittiphon, J. Seo, and S. Thanakkasaranee, (2025) *"Effect of Calcination Temperatures on Crystallite Size, Particle Size, and Antimicrobial Activity of Synthesized MgO and Its Cytotoxicity"* **International Journal of Molecular Sciences** ***26***: 4868. DOI: 10.3390/ijms26104868.